RSC Advances

PAPER

View Article Online
View Journal | View Issue

Cite this: *RSC Adv.*, 2015, **5**, 6652

Palladium nanoparticles on β-cyclodextrin functionalised graphene nanosheets: a supramolecular based heterogeneous catalyst for C–C coupling reactions under green reaction conditions†

Chandrababu Putta,‡[a] Vittal Sharavath,‡[abc] Suprabhat Sarkar[a] and Sutapa Ghosh*[ab]

Received 11th November 2014
Accepted 16th December 2014

DOI: 10.1039/c4ra14323j

www.rsc.org/advances

The use of functional properties of native cyclodextrins in palladium nanoparticle–β-cyclodextrin–graphene nanosheet (Pd@CD–GNS) catalyzed carbon–carbon (C–C) coupling reactions have been investigated under green reaction conditions. The supramolecular catalyst was prepared by deposition of Pd nanoparticles (Pd NPs) on CD–GNS using ethanol as the greener solvent and *in situ* reducing agent. The catalyst was characterised by FTIR, XRD, RAMAN, UV-Vis spectroscopy, TEM, SAED, XPS and ICP-AES. The catalytic activity of these catalysts is investigated in C–C coupling reactions such as Suzuki–Miyaura and Heck–Mizoroki reactions of aryl bromides and aryl chlorides containing functional groups under green reaction conditions *i.e.* in water, under phosphine free and aerobic conditions. This catalyst afforded excellent selectivities for the products in good to excellent yields under low Pd loadings (0.2–0.05 mol%), while ensuring the recovery and reusability of the catalysts. The reused catalyst was characterized by FTIR, TEM, XPS and ICP-AES. The CD supramolecular mediators loaded on GNS act as stabilising agents for the Pd NPs. The excellent catalytic activity of this system was attributed to the presence of CDs, excellent dispersibility in water, hydrophobic nature of the GNS support for the accumulation of organic substrates in water, "Breslow effect", the presence of PTC to overcome the mass transfer limitation onto the surface of GNS and formation of ternary CD/substrate/additive complexes on the Pd–GNS surface.

1. Introduction

Palladium (Pd) catalyzed C–C cross-coupling reactions have been the most fundamental reactions for the synthesis of various industrially important organic frameworks over the past three decades.[1–10] Although a plethora of methods and reagents have been developed by considering conventional catalytic conditions, until recently the utilization of green chemistry approaches has been of pivotal importance in the light of contemporary design of synthetic processes.[11,12] With the recent attention directed at this interface, C–C coupling reactions in aqueous medium have emerged as a major theme in catalysis research.[13] The use of highly flammable organic solvents in organic reactions is the drawback for the industrially important reactions. Hence, the use of such solvents is better to avoid or minimise. Further, the better solution is to use water as the green solvent.[14] In fact, there is a shortage of general efficient methods for cross-couplings of cheaper aryl bromides and aryl chlorides conducted in neat water under aerobic conditions and in the absence of ligands, which usually lead to lower yields and selectivities of the required product.[14a]

On the other hand, with today's focus on environment-guided processes, a promising and elegant approach would be the one bridging principles of supramolecular and green chemistry towards the preparation of cyclodextrin (CD) based active scaffolds for aqueous nanocatalysis.[15] Recent developments have been reported on the use of surface polarized supports (hydrophilic as well as hydrophobic) to immobilize metal nanoparticles and promote the catalytic activity in water.[16] Indeed, the performance of the catalyst seems to be related to the hydrophobic effect of water and suitable interactions between substrate and support. In this context, various carbon materials modified with hydrophilic molecules constitute environmentally friendly and more biocompatible

[a]*Nanomaterials Laboratory, Inorganic and Physical Chemistry Division, CSIR-Indian Institute of Chemical Technology, Hyderabad-500 607, India. E-mail: sghosh@iict.res.in; Fax: +91-40-27160921; Tel: +91-40-27191385*

[b]*RMIT Centre, CSIR-Indian Institute of Chemical Technology, Hyderabad-500607, Telangana, India*

[c]*Academy of Scientific and Innovative Research (AcSIR), New Delhi, India*

† Electronic supplementary information (ESI) available: Synthesis of CD–GNS, ^{1}H NMR and ^{13}C NMR spectra of products. See DOI: 10.1039/c4ra14323j

‡ P.C.B. and V.S. contributed equally to the study.

alternatives. Further, they can exhibit a range of fascinating properties dictated by supramolecular associations which facilitate controlled growth and aqueous dispersion of metal nanoparticles.[17–19]

Besides, graphene with a high specific surface area has great potential in the development of new kinds of composite materials, especially as a substrate to host metal nanoparticles.[20–22] However, only a few studies have involved the application of graphene-based materials as heterogeneous catalysts.[23] These oxygen functionalities make GO surface is highly hydrophilic and can stabilize the dispersion of the GO sheets in water and facilitate the deposition of Pd NPs onto the GO surface.[24] However, such functionalities on the surface may have negative effect on the accumulation of hydrophobic organic substrates on the surface of the catalyst, while conducting reaction in water as the solvent. Because of the variation in the structural arrangement of carbon atoms from a planar sp^2-hybridized geometry in graphene to a distorted sp^3-hybridized geometry in GO. Due to this reason the use of aqueous-organic solvent mixture is preferred for the utility of Pd–GNS as heterogeneous catalysts.[23o] Thus, prior to the application of Pd/RGO composites in water mediated reactions, it is essential to modify the RGO and Pd surfaces and, consequently, improve the polarity of Pd/RGO composites, to enhance the dispersion of Pd/RGO composites in a variety of solvents and finally increase the catalytic activity. In an alternative way to treat the above problems, it is possible to deposit the Pd NPs on CD–GNS support. In the endeavour to extend our research on water mediated C–C coupling reactions by using Pd on carbon as green catalysts,[25] we thought it is of interest to investigate various C–C coupling reactions such as Suzuki–Miyaura and Heck–Mizoroki coupling reactions in the presence of Pd NPs on cyclodextrin supramolecule functionalised graphene nanosheets (Pd@CD–GNS) under green reactions conditions. The pre addition of CD molecules into GO suspension, before GO was fully reduced, and the so formed CD–GNS hybrids exhibits high dispersibility and stability in water.[26] Here, we show that Pd NPs can be finely dispersed on CD–GNS by a facile route using ethanol (EtOH) as the greener solvent and *in situ* reducing agent for $PdCl_2$ in the presence of CD–GNS. Further, in order to explore the potential of CDs as supramolecules in Suzuki–Miyaura and Heck–Mizoroki reactions and from the standpoint of heterogeneous catalysis, we report here the Pd@CD–GNS catalyzed cross-coupling of various aryl bromides and aryl chlorides under green reaction conditions.

2. Experimental section

2.1. Typical procedure for Pd@CD–GNS preparation

To obtain the Pd@CD–GNS composites, 60 mg of CD–GNS was dispersed in 30 mL of EtOH by ultrasonic treatment for 1 h. To this suspension, 12 mg of $PdCl_2$ was added and the mixture was heated at 80 °C for 1 h with continuous stirring. The reaction mixture was cooled at room temperature and the solid sample with Pd loading was collected by filtration, washed extensively with EtOH and water and air dried in oven at 60 °C. ICP-AES analysis showed that 6.2 wt% of Pd was loaded in the Pd@CD–GNS catalyst.

2.2. Catalytic reactions

2.2.1. Suzuki–Miyaura cross coupling reaction. The CD–GNS supports are prepared according to the previous report as demonstrated in ESI.† Typically, the Pd@CD–GNS catalyst (3 mg, 0.2 Pd mol% *vs.* aryl halide) was placed in a 10 mL glass flask with 3 mL of H_2O and sonicated at ambient temperature (25 °C) for 10 min. The aryl halide (1.02 mmol), phenyl boronic acid (0.85 mmol) and Na_2CO_3 (1.275 mmol) were added to the resulting black suspension and the reaction mixture was heated to 90 °C for the required time. The extent of the reaction was monitored by TLC. The reaction mixture was cooled at 0 °C for 1 h, filtered and the solid washed with ethyl acetate (5 × 10 mL). The combined organic layers were separated, dried over anhydrous Na_2SO_4 and concentrated under reduced pressure. Purification of the product was done by column chromatography (250–400 mesh silica gel) using hexane or mixture of ethyl acetate and hexane as eluent to get the desired products. The identities of the products were confirmed by ^1H and ^{13}C NMR spectra of the products.

2.2.2. Heck–Mizoroki cross coupling reaction. In a typical reaction, the Pd catalyst (3 mg, 0.05 Pd mol% *vs.* aryl halide) was added to a 10 mL glass flask containing 5 mL of H_2O, aryl halide (3.4 mmol), alkene (4.08 mmol), Na_2CO_3 (5.1 mmol) and TBAB (5.1 mmol). The reaction mixture was heated at 90 °C and stirred for the required time. The extent of reaction was monitored by TLC. After the completion of the reaction, the reaction mixture was worked up using the procedure as described in Suzuki–Miyaura reaction.

3. Catalyst characterizations

The absorbance of *in situ* synthesized Pd NPs was investigated using Varian Cary 5000 UV-Vis-NIR spectrophotometer in the wavelength region between 300 to 600 nm at a resolution of 2 nm. The FT-IR (Fourier transform infrared) spectra were recorded on a BRUKER ALPHA T spectrometer from 4000 cm^{-1} to 400 cm^{-1} as KBr disks. Powder X-ray diffraction (XRD) measurements were recorded on a Siemens/D-5000 X-ray powder diffractometer using Cu Kα radiation (λ = 1.5406 Å) with scattering angles (2θ) of 2–80°. A Philips Tecnai G^2 FEI F12 transmission electronic microscope (TEM) equipped with selected area electron diffraction (SAED) operating at 80–100 kV was used for the morphological and size analyses of Pd@CD–GNS. Samples were prepared by placing one drop of an EtOH suspension of the Pd@CD–GNS hybrid composite onto a copper grid coated with carbon film. XPS analysis was carried out on a KRATOS AXIS 165 with a dual anode (Mg and Al) apparatus using the Mg Kα anode. The Pd content of the samples were determined quantitatively by inductively coupled plasma atomic emission spectroscopy (ICP-AES) using a Thermo Electron Corporation IRIS Intrepid II XDL instrument. ACME 100–200 mesh silica gel was used for column chromatography and thin layer chromatography was performed on Merck precoated silica gel 60-F254 plates. ^1H and ^{13}C NMR spectra were recorded

on a Bruker Avance spectrometer (^{1}H NMR at 300 MHz and ^{13}C NMR at 75 MHz) using $CDCl_3$ or d_6-DMSO as solvent and TMS as an internal standard. All the reactants were commercially available and used without purification. Millipore water was used for making all the solutions (18.2 MΩ, 10 ppb TOC).

4. Results and discussion

The reduction of Pd(II) ions and the deposition of PdNPs was monitored by the UV-visible spectral analysis in the presence of EtOH as solvent and reducing agent. EtOH is used as the solvent, because it is widely considered as the greener solvent in comparison to many organic solvents.[27] It is also demonstrated that $PdCl_2$ can be reduced to Pd NPs using variety of reducing agents such as hydrazine, ammonia, $NaBH_4$ which are toxic and difficult to handle. A shortcoming of these methods can be achieved by using EtOH as the greener solvent and *in situ* reducing agent.[25,28] Fig. 1 showed the UV-Vis spectrum of reaction mixture ($PdCl_2$ solution and CD–GNS in EtOH) with respect to time. The usual peaks at 420 nm at one min indicate the presence of the Pd(II) ions in reaction mixture.[29] The peaks that represent the Pd(II) ions is found to disappear over extended reaction time. The intensity at 420 nm is decreased after 1 h of the reaction time, mean while an absorbance peak appeared and apparently increased at 325 nm, which indicates the formation of Pd NPs. This indicates that Pd(II) was still present in the reaction mixture, which is attributed to the weak reducing nature of ethanol. Obtained Pd@CD–GNS catalysts were collected by centrifugation under extensive washings with water, followed by small amount of acetone to remove all unreduced Pd(II) ions of $PdCl_2$.

Fourier Transform Infrared Spectroscopy (FTIR) of CD–GNS, Pd@CD–GNS, used Pd@CD–GNS for Suzuki–Miyaura and Heck–Mizoroki reactions are shown in Fig. 2. It is found that the FTIR spectrum of CD–GNS (Fig. 2a) exhibits the C=C conjugation (in the range of 1540–1575 cm^{-1}) and C–C band (in the range of 1195–1215 cm^{-1}) of GNS, and typical CD absorption

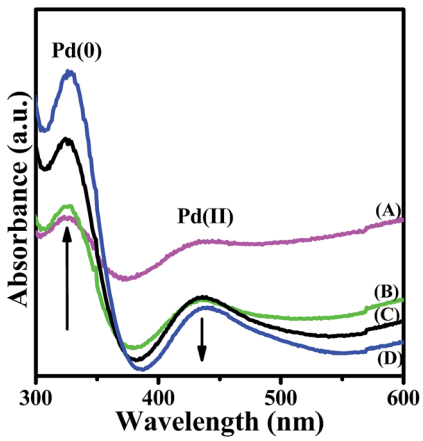

Fig. 1 Representative UV-Vis spectra of reaction mixture ($PdCl_2$ in EtOH in the presence of CD–GNS) monitored at 1 (A), 15 (B), 30 (C), and 60 min (D). The solution was refluxed at 80 °C and spectra are recorded at 30 °C.

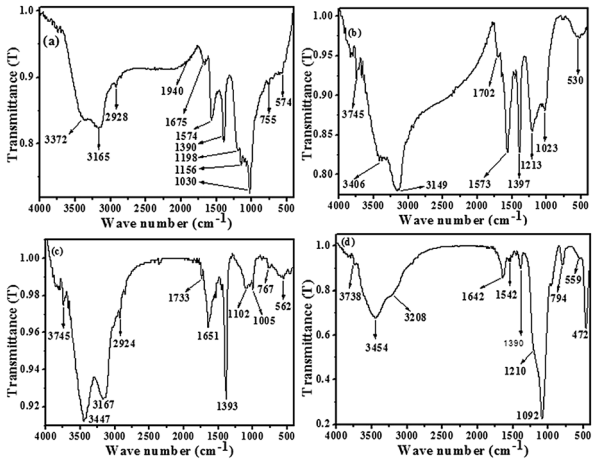

Fig. 2 FTIR spectra of the CD–GNS (a), fresh Pd@CD–GNS (b), reused Pd@CD–GNS for Heck–Mizoroki reaction (after 2 runs) (c) and reused Pd@CD–GNS for Suzuki–Miyaura reaction (after 2 runs) (d).

features of the ring vibrations at 530–800 cm^{-1}, the coupled C–O–C/C–O/C–C stretching/O–H bending vibrations in the range of 1000–1160 cm^{-1}, CH_2 stretching vibrations in the range of 2920–2930 cm^{-1}, C–H/O–H bending vibrations at 1390–1400 cm^{-1}, and O–H stretching vibrations in the range of 3149–3454 cm^{-1}.[26,30]

Furthermore, the interaction between Pd NPs and CD was evidenced by FTIR spectra from the decreased relative intensity of the band at 500–800 cm^{-1} which was interpreted as the interaction force with CD that prevented the skeletal, ring breathing and pyranose ring vibration (Fig. 2b). The IR data of used catalysts for Suzuki–Miyaura coupling reaction (Fig. 2c) and Heck–Mizoroki reaction (Fig. 2d) are in accordance with the IR data of CD–GNS (Fig. 2a) and Pd@CD–GNS (Fig. 2b). Based on this, we have confirmed that CD molecules are remaining attached to the surface of GNS after reaction. From FTIR spectrum of used catalysts, it is verified that an important amount of CD was always adsorbed on the Pd–GNS surface after several washings of catalysts with water followed by small amount of acetone. On the basis of these results, it is confirmed that the catalytic conditions such as use of base (Na_2CO_3) and TBAB did not result in any loss of CDs from GNS support, indicating that the integrity of the Pd@CD–GNS hybrid structure was maintained. The CD molecules were covered on the surface of GNS and could prevent the excess leaching and aggregation of Pd NPs. The interaction between CDs and GNS was evidenced from the well redispersion of used catalyst in water. This is further confirmed by Transmission Electron Microscopy (TEM) and X-ray diffraction (XRD) analysis.

Fig. 3a showed the TEM image of CD–GNS, illustrating the flake like morphology of the catalyst support and Fig. 3b showed the TEM image of Pd@CD–GNS.[31] The CD–GNS were decorated uniformly by the Pd NPs, which ranged in size from 5–15 nm, the distribution of Pd NPs on the outer surface of CD–GNS support was homogeneous. The TEM image of used Pd@CD–GNS catalyst after two cycles of the Suzuki–Miyaura and Heck–Mizoroki reaction are shown in Fig. 3c and d,

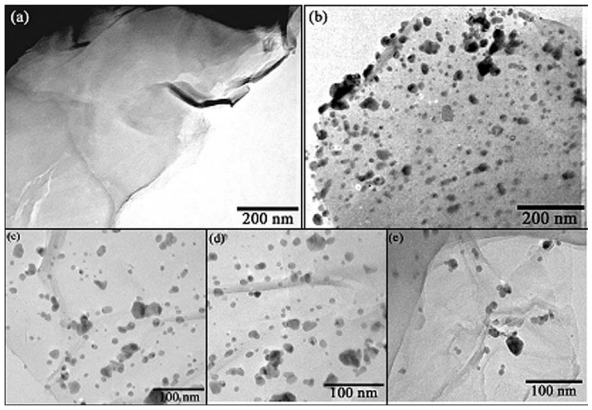

Fig. 3 TEM images of CD–GNS (a), fresh Pd@CD–GNS (b), reused catalyst for Suzuki–Miyaura reaction (after 2 runs) (c), reused catalyst for Heck–Mizoroki reaction using Na_2CO_3 as the base (after 2 runs) (d) and reused catalyst for Heck–Mizoroki reaction using NaOMe as the base (after 2 runs) (e).

respectively In order to further investigate the stability and redeposition of Pd NPs on CD–GNS after the catalytic tests, used Pd@CD–GNS catalysts in the presence of two bases such as Na_2CO_3 and NaOMe were characterized using TEM after the catalytic reaction. This shows that Pd NPs are still having similar size as in the fresh catalyst. The presence of Pd NPs on CD–GNS for the reused catalyst (2 times) was fewer compared to the fresh catalyst (Fig. 3d). The above results reveal that the present method can produce well stabilized Pd NPs on CD–GNS supports upto four cycles. It is assumed that the Pd NPs are physically adsorbed on GNS at the regions of CD through probable hydrophobic interactions which limit the mutual coalescence of Pd NPs.[32] Although, hydrophobic interactions between Pd NPs and CD are evidenced, it is crucial to definitively rule out other interactions from carbon vacancies, defects, and epitaxial absorption.[33]

The XRD pattern of the as-synthesized Pd@CD–GNS is shown in Fig. 4. The diffraction peak at ~24° is attributed to the (002) reflection of the GNS structure, the reflection is consistent with a graphene-based composite.[34] The Bragg reflections in the XRD pattern were observed at 40.2°, 46.6°, and 68.2° correspond to the (111), (200) and (220) planes of a face-centered cubic (fcc) lattice (JCPDS no. 46-1043), respectively, indicating the Pd NPs synthesized in this study have the fcc crystal structure.[33] Using the Pd (111) diffraction peak and Scherrer's equation, the mean crystallite size of the Pd NPs in the as obtained hybrids was calculated to be ~12 nm. Furthermore, the selected area electron diffraction (SAED) pattern, shown in Fig. 5, indicated that the Pd NPs were well deposited on CD–GNS, consistent with the result obtained from the TEM image (Fig. 3b).[35,36] The polycrystalline nature of Pd NPs produced four diffraction rings in sequence from inner to outer and can be indexed to the (111), (200), (220), and (311) of the fcc Pd planes, respectively, which is consistent with the result obtained from the XRD pattern.

The high-resolution X-ray photoelectron spectroscopy (XPS) narrow scan investigation of the fresh Pd@CD–GNS catalyst showed that Pd is present in the zero oxidation state (Fig. 6). The observed binding energy peaks of Pd $3d_{5/2}$ at 335.3 eV and Pd $3d_{3/2}$ at 340.8 eV ($\Delta = 5.5$ eV) clearly indicate the presence of Pd(0) in the Pd@CD–GNS catalyst (Fig. 6a).[34,37]

The XP spectrum of the catalyst after being recycled for three times in the Heck reaction shows the presence of additional peaks at 337.0 eV and 343.0 eV ($\Delta = 6.0$ eV) corresponding to Pd 3d doublet of Pd(II) at higher binding energy (Fig. 6b), which can be attributed to the slight conversion of Pd(0) to Pd(II). The presence of very small amount of Pd in its unreduced form on CD–GNS support might be due to the complexation of Pd(II) with the oxygen functionalities of the GNS support and the weak reducing nature of EtOH.[25a]

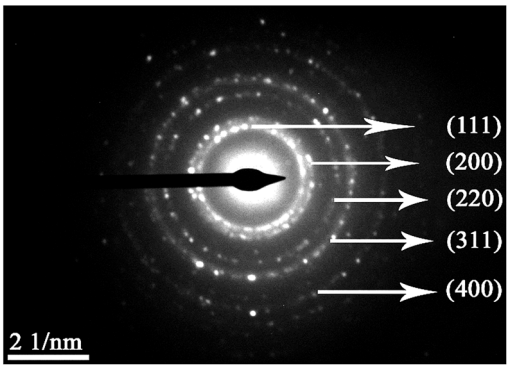

Fig. 5 Electron diffraction pattern of Pd@CD–GNS.

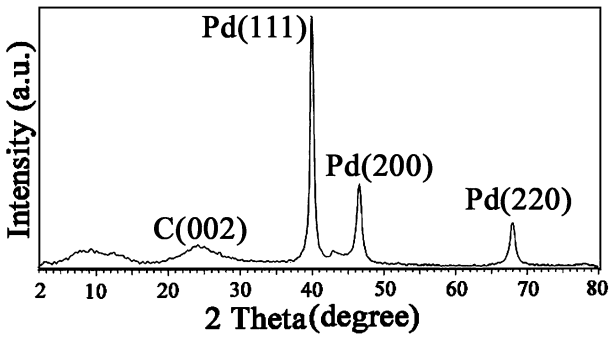

Fig. 4 XRD pattern of Pd@CD–GNS.

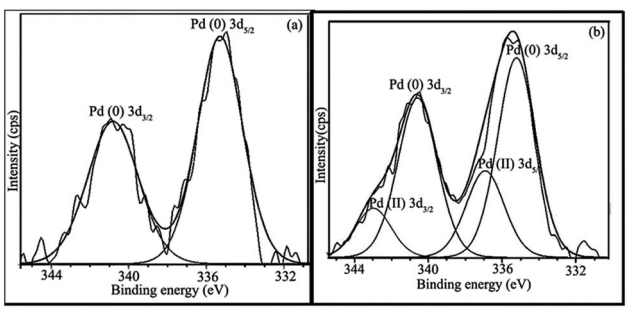

Fig. 6 XPS spectrum of the Pd@CD–GNS hybrid catalysts (a), reused catalyst for Suzuki–Miyaura reaction (after 2 runs) (b).

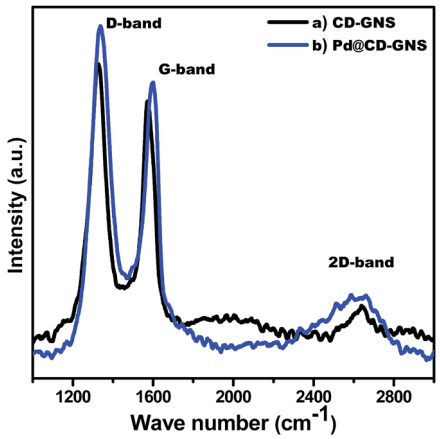

Fig. 7 Raman spectra of CD–GNS and Pd@CD–GNS samples.

The Raman spectra of CD–GNS and Pd@CD–GNS are shown in Fig. 7. The two bands at about *ca.* 1580 cm^{-1} and *ca.* 1330 cm^{-1} correspond to the in-phase vibration of the graphene lattice (G band) and the disorder induced D band, respectively. Further, it can be noted that the G band is assigned to the E_{2g} phonon of the sp^2 carbons and the D band is a breathing mode of the κ-point phonons of A_{1g} symmetry. The spectra show an obvious blue shift of the D band from ~1328 cm^{-1} (Fig. 7a) to ~1337 cm^{-1} (Fig. 7b).

This blue shift is observed due to the loading of Pd NPs by reduction of Pd^{+2} under mild chemical condition in ethanol. The spectra of CD–GNS and Pd@CD–GNS also show blue shifted G band at ~1573 cm^{-1} and ~1598 cm^{-1}, respectively. High $I(D)/I(G)$ intensity ratios are associated with high degree of disorder/exfoliation. The D/G ratios for CD–GNS and Pd@CD–GNS were calculated to be *ca.* 1.125 and 1.180, respectively. Further, the $I(D)/I(G)$ intensity ratio of Pd@CD–GNS is higher than that of CD–GNS. Such an enhancement clearly indicates chemical interaction between the Pd NPs and CD–GNS. The minimal increase in the D-band intensity may be due to the loading of Pd on CD–GNS that may create minimal defects in CD–GNS.[33] We have also observed high-energy second-order 2D-bands for CD–GNS and Pd@CD–GNS samples at ~2641 cm^{-1} and ~2620 cm^{-1}, respectively, which is associated with the local defects. A 2D band, which is the characteristic band of graphene, is generally used to identify the number of layers of graphene in the material. These 2D bands indicate that the nanosheets contain only a few layers of graphene.[25b]

The introduction of CD molecules into GO, before GO was fully reduced resulted CD–GNS hybrids exhibited high dispersibility and stability in water, and do not aggregate for a long time. Because of these versatile properties, CD–GNS supported Pd NPs have been investigated as recyclable heterogeneous Pd catalysts in pure water. Due to the dispersibility of Pd@CD–GNS, the C–C coupling reactions are performed in pure water and with easy work-up procedure after reaction completion. The catalytic activity and recyclability of the Pd@CD–GNS were also investigated for Suzuki–Miyaura reactions of several aryl bromides and aryl chlorides containing a wide range of functional groups using water as the solvent and with low catalyst loadings (0.2 mol%). The reaction between *p*-chlorobenzaldehyde and phenyl boronic acid in water gave a 90% isolated yield of the coupled product after 3 h at 90 °C in air (Table 1, entry 7).

We obtained good to excellent yields with variety of aryl chlorides having different substituents. It was also observed that aryl chlorides and bromides with hydrophilic substituents produced higher yields, while chlorides with hydrophilic substituents gave excellent yields and can be attributed to the high solubility of substrates in water (Table 1, entries 3 and 10). CD molecules present on the GNS hydrophobic surface not only stabilize the nanoparticles during the reaction, but also act as supramolecules to improve the catalytic efficiency. This, therefore provides an environment for hydrophobic guest molecules in water. The driving force for the hydrophobic guest molecules to diffuse onto the CD–GNS is mainly ascribed to the hydrophobic–hydrophobic interaction in water.[25] The organic substrates with hydrophobic substituents also afforded good to excellent yields of product. These good yields are due to "Breslow effect" and the hydrophobic nature of the support, as well as stabilization of reactive leached Pd species on the support in water.[38–40] Aryl bromides and simple aryl chlorides afforded good to excellent yields in pure water (Table 1, entries 1–6). The reaction with boronic acid other than $PhB(OH)_2$ also gave good yields (Table 1, entry 5). We performed a reaction with 2-pyridyl chloride in water, which afforded an excellent yield of about 85% after 4.5 h (Table 1, entry 12) (Scheme 1).

Furthermore, the catalytic activity and recyclability of the Pd@CD–GNS were also investigated in the Heck–Mizoroki cross coupling of aryl bromides and aryl chlorides with olefins in water and under low catalyst loading (0.05 mol%). In the presence of TBAB as a phase transfer catalyst (PTC), the coupling of bromobenzene with styrene was initially studied as a model reaction. To optimize the reaction conditions, a series of experiments with different quantities of Pd@CD–GNS hybrid

Table 1 Suzuki–Miyaura cross coupling reaction of aryl halides with phenyl boronic acid by Pd@CD–GNS in H_2O[a]

Entry	R	X	Yield[b] (%)	Time (h)
1	H	Br	93, 88[c], 85[d]	3, 3[c], 4.5[d]
2	CHO	Br	96	2
3	OH	Br	90	3
4	Me	Br	90	3.5
5	NO_2[e]	Br	88	2
6	H	Cl	90	3.5
7	CHO	Cl	90	3
8	Me	Cl	86	4.5
9	OMe	Cl	90	4.5
10	OH	Cl	90	4
11	NO_2	Cl	92	3
12	2-Pyridyl	Cl	85	4.5

[a] Reaction conditions: aryl halide (0.85 mmol), phenyl boronic acid (1.02 mmol), Na_2CO_3 (1.275 mmol), Pd@CD–GNS (3 mg, 0.2 mol% *vs.* aryl halide) and 5 mL of H_2O, under air, heated at 90 °C. [b] Isolated yield was determined by ^1H NMR. [c] Using K_3PO_4 as base. [d] 0.05 mol% of Pd loading was used. [e] 4-Nitro phenyl boronic acid was used instead of $PhB(OH)_2$.

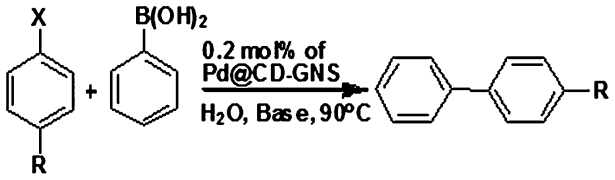

Scheme 1 Suzuki–Miyaura cross coupling reaction of aryl halides with phenyl boronic acid by Pd@CD–GNS in H_2O.

catalyst were carried out at 90 °C in water and in the presence of TBAB, the results of which are shown in Table 2. Under these reaction conditions, it was found that the best result in terms of yield and selectivity was obtained by using 0.05 mol% of Pd@CD–GNS (Table 3, entry 3). It is found that the increase in the catalyst loading to 0.2 mol% resulted a significant drop in yield to 30%. The use of low Pd loadings leads to a marked improvement in the yield and selectivity of the Heck–Mizoroki cross coupled product.[41,42] The use of optimum Pd catalyst loadings leads to a marked improvement in the yield and selectivity of the Heck–Mizoroki cross coupled product is due to the presence of the catalyst in "homeopathic dose".[43] Interestingly, the use of sodium methoxide (NaOMe) as the base affords good yields which may be due to the presence of a small amount of methanol that is formed from the hydrolysis of NaOMe. The, so formed methanol can act as the *in situ* reducing agent to reduce Pd(II) for regenerating the catalyst (Table 2, entry 10). But, *in situ* formed NaOH causes the aggregation of the Pd NPs.

Table 2 Heck–Mizoroki cross coupling reaction of aryl halides with alkenes by Pd@CD–GNS in H_2O[a]

Entry	R_1	X	R_2	Yield[b] (%)	Time (h)
1	H	Br	Ph	80[c], 76[d] 72[e], 70[f] 70[g], 52[h]	24[c], 24[d] 24[e], 24[f] 24[g], 24[h]
2	H	Br	COOMe	86	24
3	CHO	Br	Ph	80, 4–8[i]	22, 24[i]
4	H	Br	COO*t*Bu	85	24
5	Me	Br	Ph	75	24
6	Me	Br	COOMe	83	24
7	*t*Bu	Br	Ph	70	24
8	OMe	Br	COOH	90	22
9	OH	Br	Ph	95	15
10	CHO	Cl	Ph	75	24
11	H	Cl	Ph	70	24
12	H	Cl	COOMe	73	24
13	CHO	Cl	COOH	88	20
14	Me	Cl	Ph	60	24
15	Me	Cl	COOMe	64	24
16	OMe	Cl	Ph	66	24
17	NO_2	Cl	COOH	90	20
18	OH	Cl	Ph	95	18

[a] Reaction conditions: aryl halide (3.4 mmol), alkene (4.08 mmol), Na_2CO_3 (5.1 mmol), TBAB (5.1 mmol), Pd@CD–GNS (3 mg, 0.05 mol% *vs.* aryl halide) and 5 mL of H_2O, under air, heated at 90 °C. [b] Isolated yields. [c] Using Na_2CO_3 as base. [d] Using Et_3N as base. [e] Using NaOMe as base. [f] Using KOH as base. [g] Using K_3PO_4 as base. [h] Using NaOAc as base. [i] Reaction performed without TBAB.

Table 3 Effect of the catalyst loading in Heck–Mizoroki cross coupling reaction of bromobenzene with styrene by Pd@CD–GNS in H_2O[a]

Entry	Pd loading (mol% *vs.* bromobenzene) (mmol)	Yield[b] (%)	Selectivity[c] (Heck product/ biphenyl)
1	0.2 (0.0068)	30	90 : 10
2	0.1 (0.0034)	40	94 : 6
3	0.05 (0.0017)	80	100 : 0
4	0.02 (0.00068)	75	100 : 0

[a] Reaction conditions: bromobenzene (3.4 mmol), styrene (4.08 mmol), Na_2CO_3 (5.1 mmol), TBAB (5.1 mmol), Pd@CD–GNS and 5 mL of H_2O, under air, heated at 90 °C for 24 h. [b] Isolated yields. [c] Selectivity was determined by ^1H NMR.

It is demonstrated that the presence of strong base such as KOH or NaOH has negative effect for the stability of Pd NPs.[44] The TEM image (Fig. 3e) showed that the Pd NPs deposited on CD–GNS were of increased diameter in comparison to fresh catalysts. To optimize the influence of different bases in the Heck–Mizoroki cross coupling reaction between bromobenzene and styrene, a series of experiments with different bases were carried out at 90 °C in water, using 0.05 mol% of Pd catalysts and in the presence of TBAB, and the results are demonstrated in Table 2. It was found that the best result in terms of yield and selectivity was obtained by using Na_2CO_3 as the base (Table 2, entry 1). We found that stronger bases, such as KOH, NaOMe, NaOAc, and K_3PO_4 have decreased the isolated yield to some extent. It is demonstrated that the use of strong bases has negative effect for the stability of Pd NPs.[44] This result indicates that deactivation of the catalyst is likely to involve the formation of aggregated Pd NPs which leads to the decrease in the surface area of active species. It was found that the best system for the reaction was H_2O as the solvent in combination with Na_2CO_3 as the base, which delivered 70% isolated yield of the required product after 24 h when 0.05 mol% of Pd@CD–GNS was used (Table 2, entry 1). We have also examined the coupling of other aryl bromides and aryl chlorides with olefins in the optimized conditions as mentioned above and the results are summarized in Table 2. The reaction was performed with bromobenzene also using various alkenes including styrene, acrylates and acrylic acid to get the corresponding coupled products in excellent yields and selectivities. Moreover, deactivated aryl chlorides also gave the cross coupled products in moderate yields and excellent selectivities (Scheme 2).

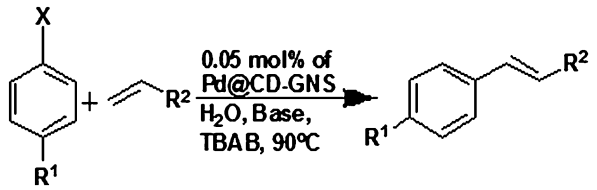

Scheme 2 Heck–Mizoroki cross coupling reaction of aryl halides with alkenes by Pd@CD–GNS in H_2O.

The use of PTC in the catalytic reaction brings the organic substrates near to the CD hydrophobic cavity and Pd NPs surfaces to perform the overall catalytic process. The CD cavity size allows the formation of a 1 : 1 : 1 substrate–surfactant–β-CD ternary complex.[45] In principle, the more hydrophobic product like stilbenes or its derivatives gets expelled from the catalyst surface at a faster rate. The high catalytic activities of these catalysts were explained high dispersibility of Pd@CD–GNS in water followed by a simultaneous interaction of organic substrates with both the CD cavity and thereby the attachment of Pd NPs to the surface of CD–GNS. The catalytic activity of this catalyst is attributed to the formation of ternary CD/substrate/additive complexes on Pd–GNS surface.[46] The high selectivities of the required product were not only attributed to the hydrophobic CD cavities but also to the influence of water solvent.[14a]

It is also demonstrated that the increase in stereoselectivity is due to the presence of the substrate into the CD cavity during β-H elimination. CD–GNS support reduces the mass transfer limitation of the reactants during the reaction, resulting in excellent catalytic activity. Further, it is demonstrated that the combination of hydrophobic nature of CD cavity as a binding site for organic substrates and a reactive centre of Pd core provides higher yields and selectivities of the required products in pure water.

We verified that the Pd@CD–GNS are recyclable for the Suzuki–Miyaura coupling reaction of 4-bromobenzaldehyde with phenylboronic acid in water and could be reused up to four cycles. The reusability of the catalyst can be explained by the redeposition of the Pd NPs on the CD–GNS upon completion of the reaction and cooling of the system. Conversion as a function of reaction time for the recycling of Pd@CD–GNS for the reaction of 4-bromobenzaldehyde with phenylboronic acid is shown in Table 4. Further, the conversion as a function of reaction time for the recycling of Pd@CD–GNS for the Heck coupling reaction of styrene with bromo benzene is shown in Table 4. The gradual decrease in activity was observed over four successive runs. For an evidence of leaching of Pd from the support during the reaction, a hot filtration test was performed for the reaction of 4-bromobenzaldehyde with phenylboronic acid. The catalyst is separated from the reaction mixture in hot condition after 20 min of the reaction time, where the isolated yield of ~30% is obtained. The reaction is further proceeded with the filtrate, which yielded ~70% of the product with increased reaction time up to 24 h. ICP-AES analysis showed that there was only a 0.31 wt% loss of Pd in the used catalyst after three cycles of the Suzuki–Miyaura reaction compared to that of the pure catalyst.

Table 4 Reusability of Pd@CD–GNS in the Suzuki–Miyaura and Heck–Mizoroki coupling reactions

No. of cycles	1	2	3	4
Suzuki reaction conversion (%)	100	98	90	84
Time (h)	2	4	5.5	8
Heck reaction conversion (%)	100	92	82	80
Time (h)	22	25	28	30

Further, the TEM image of the catalyst after two uses showed presence of redeposited Pd NPs on CD–GNS (Fig. 3c).

5. Conclusions

Remarkably, Pd NPs supported on CD–GNS were employed as a suitable and recyclable heterogeneous catalyst for the Suzuki and Heck in green solvent such as water. During the reaction in aqueous medium, all organic molecules would be strongly adsorbed on the surface of GNS because of complete hydrophobic nature of GNS surface and therefore the conversions of the reactants would be increased. Further, it is demonstrated that the combination of hydrophobic nature of CD cavity as an inclusion site for all organic molecules and the Pd NPs provides excellent yields and excellent selectivity of the products in aqueous medium. The CDs loaded on GNS act as stabilising agents for the Pd NPs to prevent agglomeration. Inspired by these major concepts of heterogeneous catalysis, supramolecular chemistry, and green chemistry, we have now explored that CDs would be successfully employed as versatile functional agents in the stabilization of metal NPs (MNPs) on GNS and those can be applied as the heterogeneous catalysts in other organic transformations in aqueous medium. Combining the advantages of metal nanoparticles (catalytically active) and CDs (supramolecular associations), the use of MNPs@CD–GNS catalysts may be explored in selective electrochemical detection of analytes, electrocatalysis such as formic acid oxidation, alcohol oxidation and sensors in near future.

Acknowledgements

P.C.B. and V.S. acknowledge CSIR, New Delhi for providing research fellowship. This work is funded by CSIR, India through SPECS, INDUSMAGIC and MULTIFUN. S.S. acknowledge Department of Science and Technology (DST), India for providing fellowship. The authors also acknowledge Dr M. Lakshmi Kantam, Director, CSIR-IICT for the support and encouragement. The authors also acknowledge Dr B. Sreedhar for the support in TEM and XPS analysis.

References

1 H. U. Blaser, A. Indolese, F. Naud, U. Nettekoven and A. Schnyder, *Adv. Synth. Catal.*, 2004, **346**, 1583–1598.
2 W. A. Herrmann, K. O. Fele, D. V. Preysing and S. K. Schneider, *J. Organomet. Chem.*, 2003, **687**, 229–248.
3 J. G. de Vries, in *Encyclopedia of Catalysis*, ed. I. T. Horvat, Wiley & Sons, New York, 2003, p. 295.
4 M. Beller and A. Zapf, in *Handbook of Organo palladium Chemistry for Organic Synthesis*, ed. E. Negishi and A. de Meijere, Wiley & Sons, Hoboken, NJ, 2002, p. 1209.
5 G. C. Fu and A. F. Littke, *Angew. Chem., Int. Ed.*, 2002, **41**, 4176–4211.
6 T. E. Barder, S. D. Walker, J. R. Martinelli and S. L. Buchwald, *J. Am. Chem. Soc.*, 2005, **127**, 4685–4696.
7 N. Kataoka, Q. Shelby, J. P. Stambuli and J. F. Hartwig, *J. Org. Chem.*, 2002, **67**, 5553–5566.

8 M. M. Manas and R. Pleixats, *Acc. Chem. Res.*, 2003, **36**, 638–643.
9 D. Astruc, F. Lu and J. R. Aranzaes, *Angew. Chem., Int. Ed.*, 2005, **44**, 7852–7872.
10 B. Cornelio, G. A. Rance, M. L. Cochard, A. Fontana, J. Sapi and A. N. Khlobystov, *J. Mater. Chem. A*, 2013, **1**, 8737–8744.
11 S. H. Huang, C. H. Liu and C. M. Yang, *Green Chem.*, 2014, **16**, 2706–2712.
12 D. Astruc, *Inorg. Chem.*, 2007, **46**, 1884–1894.
13 Y. Li, X. M. Hong, D. M. Collard and M. A. El-Sayed, *Org. Lett.*, 2000, **2**, 2385–2388.
14 (*a*) M. Lamblin, L. Nassar-Hardy, J. C. Hierso, E. Fouquet and F. X. Felpin, *Adv. Synth. Catal.*, 2010, **352**, 33–79; (*b*) C. Rohlich, A. S. Wirth and K. Kohler, *Chem.–Eur. J.*, 2012, **18**, 15485–15494.
15 (*a*) H. Bricout, F. Hapiot, A. Ponchel, S. Tilloy and E. Monflier, *Sustainability*, 2009, **1**, 924–945; (*b*) A. K. Nezhad and F. Panahi, *ACS Sustainable Chem. Eng.*, 2014, **2**, 1177–1186; (*c*) L. Liang, A. K. Diallo, L. Salmon, J. Ruiz and D. Astruc, *Eur. J. Inorg. Chem.*, 2012, 2950–2958; (*d*) V. Kairouz and A. R. Schmitzer, *Green Chem.*, 2014, **16**, 3117–3124.
16 S. S. Soomro, C. Röhlich and K. Köhler, *Adv. Synth. Catal.*, 2011, **353**, 767–775.
17 C. Hubert, A. Nowicki, A. Roucouxa, D. Landyb, B. Leger, G. Crowyn and E. Monflier, *Chem. Commun.*, 2009, 1228–1230.
18 J. Liu, J. Alvarez, W. Ong, E. Román and A. E. Kaifer, *Langmuir*, 2001, **17**, 6762–6764.
19 L. Strimbu, J. Liu, A. E. Kaifer, L. Strimbu, J. Liu and A. E. Kaifer, *Langmuir*, 2003, **19**, 483–485.
20 G. M. Scheuermann, L. Rumi, P. Steurer, W. Bannwarth and R. Mulhaupt, *J. Am. Chem. Soc.*, 2009, **131**, 8262–8270.
21 Y. Li, X. B. Fan, J. J. Qi, J. Y. Ji, S. L. Wang, G. L. Zhang and F. B. Zhang, *Nano Res.*, 2010, **3**, 429–437.
22 A. Mastalir, Z. Kiraly, A. Patzko, I. Dekany and P. L. Argentiere, *Carbon*, 2008, **46**, 1631–1637.
23 (*a*) N. A. M. Barakat and M. Motlak, *Appl. Catal., B*, 2014, **154**, 221; (*b*) A. Bragaru, E. Vasile, C. Obreja, M. Kusko, M. Danila and A. Radoi, *Mater. Chem. Phys.*, 2014, **146**, 538; (*c*) R. C. Cerritos, V. Baglio, A. S. Arico, J. L. Garcia, M. F. Sgroi, D. Pullini, A. J. Pruna, D. B. Mataix, R. F. Ramirez and L. G. Arriaga, *Appl. Catal., B*, 2014, **144**, 554; (*d*) C. Du, J. Su, W. Luo and G. Cheng, *J. Mol. Catal. A: Chem.*, 2014, **383**, 38; (*e*) Z. Huang, H. Bao, Y. Yao, W. Lu and W. Chen, *Appl. Catal., B*, 2014, **154**, 36; (*f*) Y. Li, Y. Yu, J.-G. Wang, J. Song, Q. Li, M. Dong and C.-J. Liu, *Appl. Catal., B*, 2012, **125**, 189; (*g*) T. Niu, G. L. Liu and Y. Liu, *Appl. Catal., B*, 2014, **154**, 82; (*h*) M. H. Seo, S. M. Choi, J. K. Seo, S. H. Noh, W. B. Kim and B. Han, *Appl. Catal., B*, 2013, **129**, 163; (*i*) G. Wu, X. Wang, N. Guan and L. Li, *Appl. Catal., B*, 2013, **136**, 177; (*j*) Z. Wang, G. Shi, J. Xia, Y. Xia, F. Zhang, L. Xia, D. Song, J. Liu, Y. Li, L. Xia and M. E. Brito, *Electrochim. Acta*, 2014, **121**, 245; (*k*) K. Qu, L. Wu, J. Ren and X. Qu, *ACS Appl. Mater. Interfaces*, 2012, **4**, 5001–5009; (*l*) S. S. Shendage, U. B. Patil and J. M. Nagarkar, *Tetrahedron Lett.*, 2013, **54**, 3457–3461; (*m*) Y. V. Ioni, S. E. Lyubimov, V. A. Davankov and S. P. Gubin, *Russ. J. Inorg. Chem.*, 2013, **58**(4), 392–394; (*n*) L. Rumi, G. M. Scheuermann, R. Mulhaupt and W. Bannwarth, *Helv. Chim. Acta*, 2011, **94**, 966–976; (*o*) S. Moussa, A. R. Siamaki, B. F. Gupton and M. S. El-Shall, *ACS Catal.*, 2012, **2**, 145–154; (*p*) A. R. Siamaki, A. E. R. S. Khder, V. Abdelsayed, M. S. El-Shall and B. F. Gupton, *J. Catal.*, 2011, **279**, 1–11; (*q*) W. Liu, L.-Z. Zheng, Y. Li and Q. Liu, *Fenzi Cuihua*, 2011, **25**, 549–556; (*r*) G. M. Scheuermann, L. Rumi, P. Steurer, W. Bannwarth and R. Mulhaupt, *J. Am. Chem. Soc.*, 2009, **131**, 8262–8270; (*s*) Y. Li, X. B. Fan, J. J. Qi, J. Y. Ji, S. L. Wang, G. L. Zhang and F. B. Zhang, *Nano Res.*, 2010, **3**, 429–437; (*t*) A. Mastalir, Z. Kiraly, A. Patzko, I. Dekany and P. L'Argentiere, *Carbon*, 2008, **46**, 1631–1637; (*u*) N. Li, Z. Y. Wang, K. K. Zhao, Z. J. Shi, S. K. Xu and Z. N. Gu, *J. Nanosci. Nanotechnol.*, 2010, **10**, 6748–6751; (*v*) L. Ren, F. Yang, Y. Li, T. Liu, L. Zhang, G. Ning, Z. Liu, J. Gao and C. Xu, *RSC Adv.*, 2014, **4**, 26804–26809; (*w*) L. Ren, F. Yang, C. Wang, Y. Li, H. Liu, Z. Tu, L. Zhang, Z. Liu, J. Gao and C. Xu, *RSC Adv.*, 2014, **4**, 63048–63054.
24 C. Xu, X. Wang and J. W. Zhu, *J. Phys. Chem. C*, 2008, **112**, 19841–19845.
25 (*a*) C. B. Putta and S. Ghosh, *Adv. Synth. Catal.*, 2011, **353**, 1889–1896; (*b*) S. Ghosh and V. Sharavath, *RSC Adv.*, 2014, **4**, 48322–48330.
26 Y. Guo, S. Guo, J. Ren, Y. Zhai, S. Dong and E. Wang, *ACS Nano*, 2010, **4**, 4001–4010.
27 P. G. Jessop, *Green Chem.*, 2011, **13**, 1391–1398.
28 (*a*) N. Toshlma, T. Yonezawa and K. Kushihashi, *J. Chem. Soc., Faraday Trans.*, 1993, **89**(14), 2537–2543; (*b*) X. Liu, W. Liu, J. Li, Y. Zhang, L. Lang, L. Ma and B. Zhang, *Ind. Eng. Chem. Res.*, 2010, **49**, 8826–8831.
29 M. L. Kantam, S. Roy, M. Roy, B. Sreedhar and B. M. Choudary, *Adv. Synth. Catal.*, 2005, **347**, 2002–2008.
30 H. M. Heise, R. Kuckuk, A. Bereck and D. Riegel, *Vib. Spectrosc.*, 2010, **53**, 19–23.
31 Z. Jin, D. Nackashi, W. Lu, C. Kittrell and J. M. Tour, *Chem. Mater.*, 2010, **22**, 5695–5699.
32 J. D. Senra, L. F. B. Malta, M. E. H. M. da Costa, R. C. Michel, L. C. S. Aguiar, A. B. C. Simas and O. A. C. Antunes, *Adv. Synth. Catal.*, 2009, **351**, 2411–2422.
33 (*a*) Y. Li, X. Fan, J. Qi, J. Ji, S. Wang, G. Zhang and F. E. Zhang, *Nano Res.*, 2010, **3**, 429–437; (*b*) J. Yang, C. Tian, L. Wang and H. Fu, *J. Mater. Chem.*, 2011, **21**, 3384–3390.
34 V. B. Parambhath, R. Nagar and S. Ramaprabhu, *Langmuir*, 2012, **28**, 7826–7833.
35 Z. Zhang, F. Xiao, J. Xi, T. Sun, S. Xiao, H. Wang, S. Wang and Y. Liu, *Nat. Sci. Rep.*, 2014, 4053.
36 X. Chena, W. Zangb, K. Vimalanathana, K. S. Iyera and C. L. Rastona, *Chem. Commun.*, 2013, **49**, 1160–1162.
37 G. M. Scheuermann, L. Rumi, P. Steurer, W. Bannwarth and R. Mülhaupt, *J. Am. Chem. Soc.*, 2009, **131**, 8262–8270.
38 D. C. Rideout and R. Breslow, *J. Am. Chem. Soc.*, 1980, **102**, 7816–7817.
39 R. Breslow, *Acc. Chem. Res.*, 1991, **24**, 159–164.
40 R. Breslow, U. Maitra and D. Rideout, *Tetrahedron Lett.*, 1983, **24**, 1901–1904.

41 A. H. M. de Vries, J. M. C. A. Mulders, J. H. M. Mommers, H. J. W. Henderickx and J. G. de Vries, *Org. Lett.*, 2003, **5**, 3285–3288.
42 M. T. Reetz and J. G. de Vries, *Chem. Commun.*, 2004, 1559–1563.
43 A. H. M. de Vries, J. M. C. A. Mulders, J. H. M. Mommers, H. J. W. Henderickx and J. G. de Vries, *Org. Lett.*, 2003, **5**(18), 3285–3288.
44 Z. Q. Zhou, L. H. Wu and Y. Liu, *Chemical Agent*, 2008, **30**, 729.
45 E. S. Aman and D. Serve, *J. Colloid Interface Sci.*, 1990, **138**(2), 365–375.
46 C. Torque, B. Sueur, J. Cabou, H. Bricout, F. Hapiot and E. Monflier, *Tetrahedron*, 2005, **61**, 4811–4817.